Colloid Microthruster Flight Performance Results from Space Technology 7 Disturbance Reduction System

John Ziemer [1], Colleen Marrese-Reading[2], Charley Dunn[3], Andrew Romero-Wolf[4], Curt Cutler[4], Shahram Javidnia[4], Thanh Li[4], Irena Li[4], Garth Franklin[5], and Phil Barela[6],
Jet Propulsion Laboratory, 4800 Oak Grove Drive, Pasadena, CA, 91109

Oscar Hsu[7], Peiman Maghami[7], Jim O'Donnell[7], Jake Slutsky[8], and James Ira Thorpe[8]
Goddard Space Flight Center, 8800 Greenbelt Rd, Greenbelt, MD, 20771

Nathaniel Demmons[9] and Vlad Hruby[10]
Busek Co., 11 Tech Circle, Natick, MA, 01760

and

LISA Pathfinder Team
European Space Agency

Abstract: Space Technology 7 Disturbance Reduction System (ST7-DRS) is a NASA technology demonstration payload as part of the ESA LISA Pathfinder (LPF) mission, which launched on December 3, 2015. The ST7-DRS payload includes colloid microthrusters as part of a drag-free dynamic control system (DCS) hosted on an integrated avionics unit (IAU) with spacecraft attitude and test mass position provided by the LPF spacecraft computer and the highly sensitive gravitational reference sensor (GRS) as part of the LISA Technology Package (LTP). The objective of the DRS was to validate two technologies: colloid micro-Newton thrusters (CMNT) to provide low-noise control capability of the spacecraft, and drag-free flight control. The CMNT were developed by Busek Co., Inc., in a partnership with NASA Jet Propulsion Laboratory (JPL), and the DCS algorithms and flight software were developed at NASA Goddard Space Flight Center (GSFC). ST7-DRS demonstrated drag-free operation with <10nm/√Hz level precision spacecraft position control along the primary axis of the LTP using eight CMNTs that provided 5-30 μN each with ≤0.1 μN precision. The DCS and CMNTs performed as required and as expected from ground test results, meeting all Level 1 requirements based on on-orbit data and analysis. DRS microthrusters operated for >2400 hours in flight during commissioning activities, a 90-day experiment and the extended mission. This mission represents the first validated demonstration of electrospray thrusters in space, providing precision spacecraft control and drag-free operation in a flight environment with applications to future gravitational wave observatories like LISA.

[1] ST7 DRS Payload Systems Engineer and Thruster Cognizant Engineer, JPL, M/S 321-100, AIAA Member.
[2] ST7 DRS Thruster Technologist, Electric Propulsion Group, JPL, M/S 125-123, AIAA Member.
[3] ST7 DRS Project Technologist, JPL, MS 321-251.
[4] ST7 DRS Operations Team, JPL.
[5] ST7 DRS Integration and Test Lead and IAU Cognizant Engineer, JPL, MS 138-212.
[6] ST7 DRS Project Manager, JPL, MS 321-251.
[7] ST7 DRS Dynamic Control System Team, Attitude Control Systems Engineering Branch, NASA GSFC.
[8] ST7 DRS Experiment and Data Analysis Team and members of LISA Pathfinder Science Team, NASA GSFC.
[9] Microthruster Cognizant Engineer and Micropropulsion Lead, Busek, Co., Inc., AIAA Member.
[10] Microthruster Principal Investigator and President, Busek Co., Inc., AIAA Member.

I. Introduction

The Space Technology 7 Disturbance Reduction System (ST7-DRS) was developed to demonstrate the technologies required for nanometer spacecraft position control and 'drag-free' operation capability for future missions. The primarily application is a gravitational wave observatory like the recently selected Laser Interferometer Space Antenna (LISA) for ESA's L3 flagship mission, intended for launch in 2034. Precision spacecraft control is also of interest as a distinct technology area, for use with separated-spacecraft interferometry, formation flying, and precision pointing for the next generation of space telescopes. DRS was originally selected by NASA's New Millenium Program, and has been supported by the Astronomy and Astrophysics Directorate and Physics of the Cosmos Program. ST7 DRS was hosted as a payload on the ESA LISA Pathfinder (LPF) spacecraft. It was the first validated demonstration of electrospray thruster technology in flight. It was launched in December 2015. The mission profile is illustrated in Figure 1. Commissioning operations were conducted in January 2016 to check the functionality of the DRS subsystems, including the microthrusters. LPF arrived on station at Earth-Sun L1 Lagrange point on January 22. ESA LISA Technology Package (LTP) executed its primary mission first, and then the DRS primary mission oprations were conducted during June - Decmeber 2016. Extended mission operations were conducted during several weeks from January through April 2017 with additional experiments, further characterizing the performance and capabilities of the DRS and the DRS sub-systems.

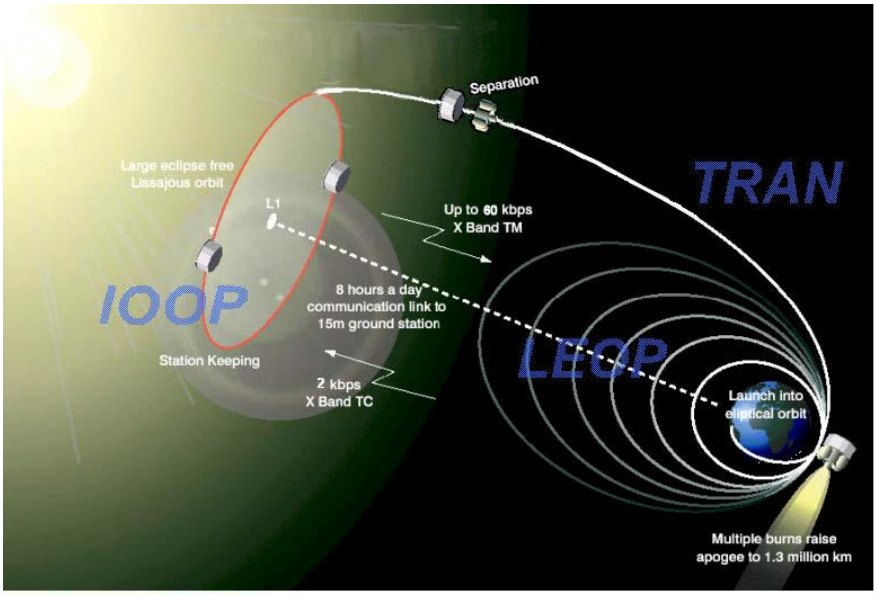

Figure 1. LISA Pathfinder and DRS Mission Profile.

The DRS consisted of four major subsystems to achieve spacecraft attitude control and drag-free operations and nanometer spacecraft position control using the gravitational reference sensor (GRS) on the LTP. It included the colloid micronewton thrusters (CMNT), Dymanic Control System (DCS), the Integrated Avionics Unit (IAU) and the command and data handing flight software (C&DH FSW). The DRS was closely coupled with the gravitational sensor provided by ESA on LPF. Drag-free spacecraft control implies a spacecraft trajectory that is affected only by external gravitational foces acting on test masses, to the the extent possible, and not by other disturbances such as solar pressure or the spacecraft itself. Precision spacecraft control wass needed to reduce noise forces from the spacecraft on the test mass. The GRS consisted of two freely floating test masses within a housing and a measurement system for determining the position of the test masses with respect to the housing and each other. In order to validate the performance of a gravitational sensor, the motion of one of the test masses must be compared to a reference trajectory provided by the other. Both test masses reside in the LTP payload and are controlled by the DRS during perionds of joint operation. The concept is illustrated in Figure 2. The time variation of the separation of the two test masses was used to determine whether external forces had been reduced to the required level necessary to enable furture gravitational wave measurement missions.

Nanometer spacecraft position control was achieved by precisely measuring the position of the spacecraft with respect to a reference test mass and actuating multiple thrusters to maintain the spacecraft trajectory following the

test mass. The test masses were intended to follow purely gravitational trajectories. In the absence of a shielding spacecraft, the test mass trajectories were affected by solar radiation pressure in addition to other forces. The spacecraft shielded the test masses from external forces but also created small disturbances of its own that had to be characterized. In the absence of a control system, solar radiation pressure would tend to push the spacecraft towards the test masses. In the steady state, the thrusters fired to exert the same force as the solar radiation pressure (plus other disturbances forces). The first use of this type of spacecraft position control was in Earth orbit, where the primary non-gravitational force was atmospheric drag, leading to the terminology for 'drag-free' control. For DRS, a multimode drag-free controller examined the attitude of the spacecraft and the position and attitude of the test masses provided by the LTP sensor to calculate applied forces and torques to the LPF spacecraft and LTP test masses. The performance of the LPF with cold gas thrusters was measured to be 5.2 ±0.1 fms-2/√Hz for frequencies between 0.7 and 20 mHz. This value is lower than the requirement for the LPF mission by 5x and within a factor of 1.25 of the requirement requirement for the LISA mission. [1] In the DRS, the position was adjusted by colloid microthrusters with submicronewton level precision. The precision spacecraft control was validated against requirements by independent measurements of the spacecraft position with respect to a second freely floating test mass.

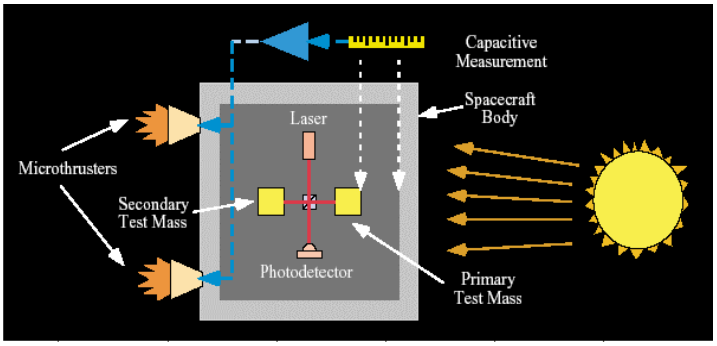

Figure 2. An illustration of the DRS concept.

The ST7 DRS technology demonstration mission had the following technology validation requirements, which constituted the project objectives:

- DRS shall demonstrate spacecraft control with 10 nm/√Hz over a frequency range of 1 mHz to 30 mHz.
- DRS shall use the LTP as its drag-free sensor
- DRS shall demonstrate a spacecraft propulsion system with noise less than 0.1 μm/√Hz over a frequence range of 1 mHz to 30 mHz
- DRS shall operate with two clusters of four thrusters each to control the spacecraft attitude for at least 60 days. An assessment of the operability of the thrusters during the period will be made including: delivered thrust, specific impulse, latencies, warm-up times, controllability, throttleability, and accuracy. This requirement was changed before launch after the propulsion system was delivered and integrated onto the spacecraft more than 6 years before the launch. The requirement was changed to any measureable thrust on-orbit.

The ST7 DRS was successful at meeting all of the project objectives during the primary mission. It demonstrated attitude and drag-free spacecraft control as planned and through transitions between different modes using colloid micronewton thrusters and the DCS for the first time in flight. Eleven experiments were conducted on the DRS over 6 months during the primary mission. During four weeks of an extended mission, fifteen more experiments were conducted. The experiments were focused on demonstrating, characterizing and improving the drag free control, thruster performance and the thruster performance model. The performance of the DRS DCS in flight in meeting the ACS and drag-free requriements on position and acceleration noise have been summarized previously [2]. This paper is focused on presenting the performance of the colloid micronewton thruster system. The configuration and operation of the DRS and the different control modes are described. The performance of the CMNT system is summarized.

II. ST7 DRS

The disturbance Reduction System consisted of 4 major subsystems in 3 units. The four subsystems included the colloid micronewton thrsuters (CMNT), Dynamic Control System (DCS), the Integrated Avionics unit (IAU) and the command and data handling flight software (C&DH FSW). They were integrated into 3 units that included the Electronics Assembly (EA) and two identical Colloid Micronewton Thruster Assemblies (CMTAs), also referered to clusters. The Electronics Asembly conisisted of the Integrated Avionics Unit (IAU) and a connector panel. The two thruster assemblies contained four microthrusters each and their corresponding electronics. An exploded view of the LISA Pathfinder spacecraft with the ST7 DRS payload is in Figure 3. DRS was a unique payload in that during operations, it controlled the spacecraft attitude and another payload, the LISA Technology Package (LTP).

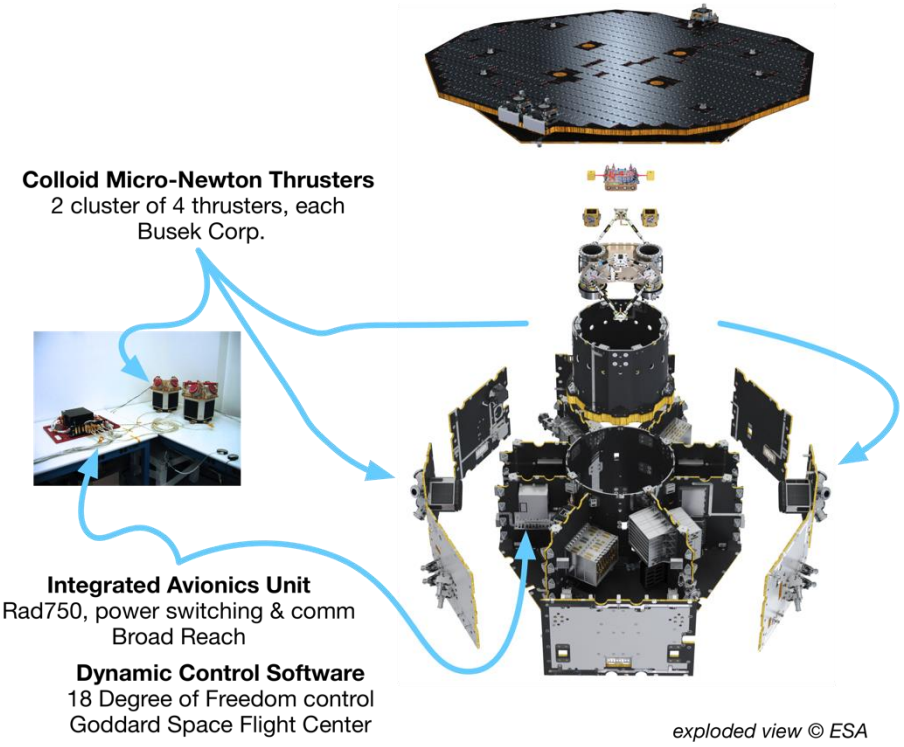

Figure 3. Exploded view of the LISA Pathfinder spacecraft with the ST7 DRS payload.

The DRS was powered by the LPF spacecraft power management system and communicateed to the spacecraft on-board computer (OBC) via serial communications connection. The DRS could be controlled by the LPF to provide a backup thruster function or control the spacecraft attitude and LTP test masses during the DRS demonstration through commands and telemetry exchanged with the OBC. The OBC on-board software (OBSW) and on-board data handing (OBDH) provided the DRS interface software and data handling. Figure 3 shows the units and assemblies of the DRS instrument. The LPF OBC, LTP Front-End Electronics, and the two Test Masses are shown in the Figure 3 also, because although external to the DRS instrument, they were necessary to the DRS experiment as the gravitational reference sensors.

A. CMNT System

The two Colloid Micronewton Thruster Assemblies (CMTAs) are identical units provided by Busek Co., Inc. A single unit with four thrusters is shown in Figure 3. A thruster assembly included: 4 thruster heads, 4 propellant feed systems, 4 Power Processing Units (PPUs), 1 cathode, and 1 Digital Control Interface Unit (DCIU). [3] The thruster head and feed systems were independently controlled through the PPUs, which were controlled, in turn by the DCIU. The DCIU had a power, command, and telemetry interface to the IAU. The DCIU also controled the cathode neutralizer. The DCIU had an on-board EPROM, which could not be reprogrammed after delivery to JPL. Each thruster head included a manifold that fed nine emitters in parallel, a heater to control propellant temperature

and physical properties, and electrodes that extract and accelerate propellant as charged droplets. The thrust from each head was throttable from 5 to 30 μN by changing the beam voltage (2-10 kV) and/or the propellant flow rate that determined the beam current (2.25-5.4 μA). A thruster electrical schematic is shown in Figure 4. Independent, fine control of both the beam voltage and beam current allow for precise control of thruster to better than 0.1 μN resolution with <0.1 μN/√Hz thrust noise. Propellant wass stored in four electrically isolated steel bellows compressed by four constant force springs set to supply four microvalves with propellant at approximarely 1 atm of pressure. The CMNT functional block diagram is shown in Figure 5. The microvalve was piezo-actuated using ~1 mW of power to control the propellant flow rate and current to better than 1 nA with out significant motion. This level of presiciosn corresponds to ≤0.01 μN of thruster, with a response time over its full range of less than 0.5 s. [4]

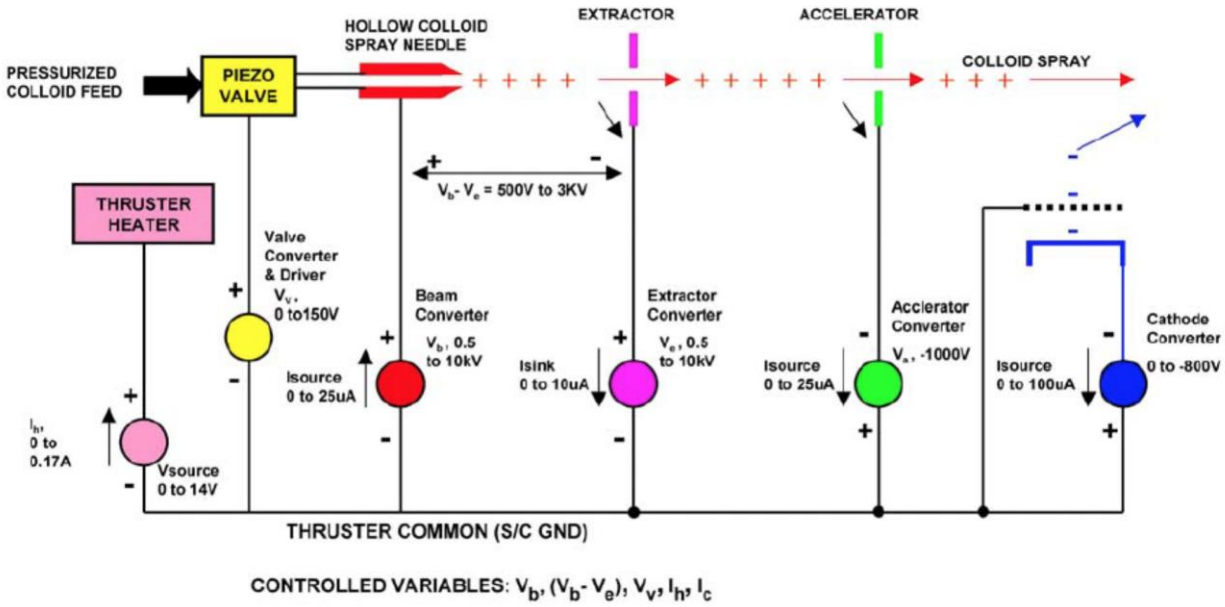

Figure 4. Thruster electrical schematic showing beam, emitter, extractor, accelerator, and cathode neutralizer voltage sources. [5]

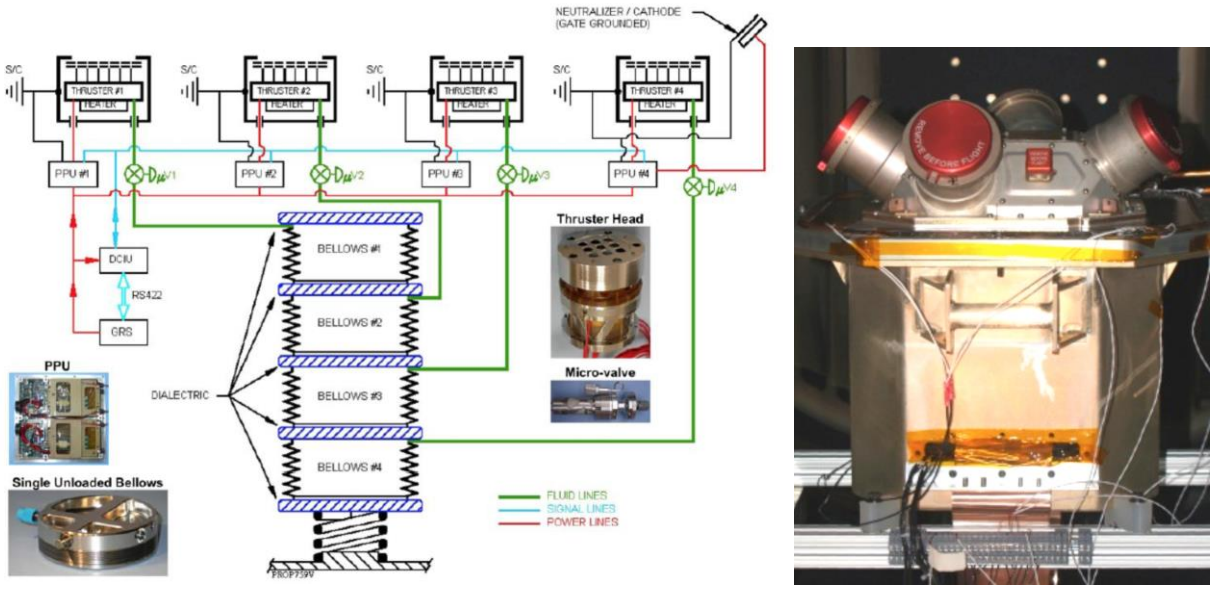

Figure 5. CMNT cluster functional block diagram [5] with pictures of various components (left) and the Busek Colloid Micro-Newton Thruster (CMNT) Flight Cluster 1 including four thruster heads, electronics, and cathode neutralizer (visible) in thermal-vacuum environmental test setup (right) [6].

The thruster performance is based on ground tests of EM units on a thrust stand, which have been used to calibrate performance models based on current and voltage measurements. Those performance models were used to

verify that the flight units met requirements since they were too heavy to be placed on a thrust stand themselves. Ground tests were conducted with EM unit thrusters for 3478 hours on a magnetically levitated thrust stand with micronewton resolution. [7] The simple model for thrust (T) in Equation 1 is based on beam current (I_B) and beam voltage (V_B) measurements and was developed and verified during ground testing with the thrust stand. The delivered thrust was achieved within 2% of the commanded thrust at nominal voltages, currents and temperature, which was the resolution of the thrust stand, and with a C_1 of 0.0319. The nominal temperature is 25°C. The nominal beam voltage is 6000 V. The nominal extraction voltage is 1600 V. The nominal current range is 2.25 – 5.3 uA. At non-nominal voltages, Taylor one losses and beam divergence effects can impact the thrust, by <2% for beam voltages between 4-8 kV and <5% for the full range of typically allowable beam voltages (2-10 kV). Temperature also influences the value of C1, which increases at colder tempertures and decreases at warmer tempertatures. The exact relation between between C1 and temperature has been predicted using models including the physical properties of the propellant and verified by measurement [8].

$$T=C_1 I_B^{1.5} V_B^{0.5} \qquad (1)$$

The cathode neutralizer, developed by Busek, was made from carbon nanotube (CNT) base with an extractor electrode. [9] The cathde was capable of producing 10 µA to 1 mA using extraction voltages of 250 to 800 V. One CNT cathodes has been tested in an ultra-high vacuum chamber for over 13,000 hours at 100 µA without incident. CNT cathodes have also been tested successfully with operating thruster heads during the pre- and post-dynamic tests and in each full functional test during the thermal environment qualification tests for each unit. Cluster 1 cathode demonstrated 13 µA at 242 V and 23 µA at 268 V in TVAC testing before flight. Cluster 2 cathode demonstrated 13 µA at 375 V and 26 µA at 420 V.

The thruster electronics included 4 power processing units (PPUs) and one digital control and interface unit (DCIU) for each cluster. They completed qualification testing at the component level and in flight assembly qualification testing [10]. EM and flight electronics have over 10,000 hours of operation under vacuum controlling complete thruster sub-systems. The PPU includes the high-voltage DC-DC converters that have been specifically designed and tesed for this application by Busek Co. The DCIU controls all four thrusters and provides the command and telemetry interface to the spacecraft and DRS flight computer.

B. DCS

The DRS Dynamic Control System (DCS) resides in the IAU and was responsible for the algorithms and flight software to control the spacecraft and the test masses by computing thruster force commands to maintain spacecraft attitude and test mass force and torque commands for drag-free operation based on spacecraft attitude and test mass positions and attidues received from the OBC. Its functions included sensor processing (from LTP and LPF), control filters propagation, actuation command generation (Thrust commands and elecrostatic actuation commands) and internal fault management. The on-board data handling (OBDH) of the OBC interacts with the DRS C&DH software on the IAU to pass commands and telemetry back and forth. The OBC stores ground commands on the MTL and telemetry from the DRS.

There are several DRS and DCS modes with different internal subsystem states within each mode. The DRS instrument enters a certain mode when the subsystems take on unique states within each mode. Each subsystem state may be commanded independently. **Initialization/Safe Mode (Init or Safe)** is the mode the DRS instrument enters upon power being applied from the spacecraft. Only the IAU had power in this mode. This was also the instrument's Safe mode. **Standby Mode** was the mode in which the DRS was not controlling either the spacecraft or the LTP test masses, and its IAU and thrusters were on but disabled. Standby mode was considered the default mode for DRS operations. **Thruster Diagnostic Mode (ThrDiag)** is the mode in which the DRS is not controlling either the spacecraft or the LTP test masses, its IAU and thrusters are on and enabled (thruster DCIU is on, PPUs are enabled) into diagnostic mode. This allows the thrusters to operate based on current and voltage commands (each thruster can be commanded independently) or thrust commands from the IAU. This mode was only expected to be used during commissioning phases or thruster fault diagnosis and recovery activities, but had to be used for most of the mission because of an anomaly in the DCIU. **Attitude Only Control Mode (AO or Att)** stabilized the attitude of the S/C and the attitude and position of test masses after handover from the LPF without compensating for solar pressure. Both test masses are were high force (wide range) mode and the DCS TM controllers were both in accel mode. Spacecraft attitude was controlled by the micro-newton thrusters. **Zero-G Mode (Acel)** mode maintained S/C and test mass states while opposing solar pressure and other secular forces acting on the S/C using the micro-newton thrusters. Both test masses were either in high force (wide range) or low force (high precision) mode and the DCS TM controllers were both in Accelerometer mode to operate the test masses as acelerometers. Spacecraft attitude

was also controlled by the micro-newton thrusters. This mode was used to measure thruster thrust levels. **Drag-Free Low Force (DFLF)** established drag-free motion about the reference test mass using the micro-newton thrusters. The reference test mass transitioned into Low-Force (high resolution) mode, with no electrostatic force commanding, although small torque commands may have been used. In this mode the spacecraft was required to center around one test mass. **18 Degrees of Freedom (18DOF)** was the second drag-free mode and the highest control mode for the DRS, controlling all 18 degrees of freedom with the highest fidelity. This was the expected mode for "science" operations with the reference test mass freely floating and the spacecraft attitude stably controlled by the colloid thrusters. In this mode, drag free motion was to be maintained for two test masses along the sensitive axis and within the DRS bandwidth.

The DCS provided both attitude and drag free control with the required performance with the colloid thrusters. It was required to maintain the spacecraft Z axis to an absolute accuracy of 2 degress (3 sigma) half cone angle with respect to the Sun vector and the rotation around the Z axis to an accuracy of 2 degress (3 sigma) with respect to the steering law. It was required to maintain the spacecraft position with respect to the test masses, about the sensitive axis (x-axis of the LTP housing frames H1 or H2), to better than 10 nm/√Hz in the measurement bandwidth (MBW). The measurement bandwidth covers the frequency range of 1 mHz to 30 mHz. It was required to maintain the spacecraft position with respect to either test mass, about the H1Y(or H2Y), to better than 30(1+f/(3 mHz)2) nm/√Hz in the MBW. It was required to maintain the spacecraft position with respect to either test mass, about the H1Z(or H2Z), to better than 30(1+f/(3 mHz)2) nm/√Hz in the MBW. The performance of the DRS in meeting all off these these requirements is presented elsewhere [2] with this paper focusing on the performance of the CMNT thrusters.

III. CMNT Flight Performance

The performance of the CNMT were characterized during commissioning and primary and extended mission phases in different modes and experiments. The critical thruster performance demonstrated in flight is summarized in Table 1 with requirements and ground test results for comparison and then discussed in more detail in the sections that follow. The thrusters performed as expected and required in flight, as they did on the ground, except that Thruster 1 had a slower response time and higher noise level. Despite the compromised thruster 1 performance, the DRS system delivered the required performance.

Table 1. CMNT performance requirements and performance summary.

Performance Parameters	**ST7 Requirement**	**Ground Tests**	**Demonstrated in Flight**							
			Thr 1	**Thr 2**	**Thr 3**	**Thr 4**	**Thr 5**	**Thr 6**	**Thr 7**	**Thr 8**
Thrust Range (μN)	5 to 30	4.35 to 35.8	5-30	**5-50**	5-30	5-30	**5-60**	5-30	5-30	5-30
Thrust Precision (μN)	≤0.1	0.08 (0.01 calculated)	##	≤0.1	≤0.1	≤0.1	≤0.1	≤0.1	≤0.1	≤0.1
Thrust noise (μN/√Hz)	≤0.1	≤0.01 ($3x10^{-5}$ to 3 Hz) <0.1 (3-4 Hz)	≤0.8	≤0.1	≤0.1	≤0.1	≤0.1	≤0.1	≤0.1	≤0.1
Thrust Range Response Time (s)	≤ 100 s	< 10 s	147 s on thruster #1)	<10 s	<10 s	<10 s	<10 s	<10 s	<10 s	<10 s
Operational Lifetime (hours)	any measurable thrust on-orbit*	3478 hours during FLT 2B (245 Ns of impulse, 113 g of propellant)	>2400 hrs (100 days)	>2400 hrs (100 days)	>2400 hrs (100 days)	1690 hrs, (70 days)	>2400 hrs (100 days)	>2400 hrs (100 days)	>2400 hrs (100 days)	>2400 hrs (100 days)
Propellant mass sprayed (grams)		113	74.8	67.02	84.1	68.89	64.46	59.05	91.07	89.52

* Given the unplanned 7+ years they sat after delivery. Goal was ≥2160 hours (90 days).

C. Thrust Range

The CMNT performance was verified in flight and was consistent with performance data from ground tests. The ground and flight performance are presented in Table 1. Commanded and calucated thrust levels are presented in Figure 6 for each of the 8 thrusters in the required 5-30 µN thrust range. The thrust levels are calculated from measured current and voltage and the thrust model in Eqn 1. Thruster 1 did demonstrate the full thrust range, however it required ≤147 s, instead of 10 s as demonstrated by the other thrusters. In the extended mission, higher than nominal thrust levels were explored to demonstrate the capability. Thrusters 2 and 5 were stepped up to 40 µN early in the extended mission and then they were stepped up to 50 and 60 µN in the last week of the extended mission. These data are in Figure 7.

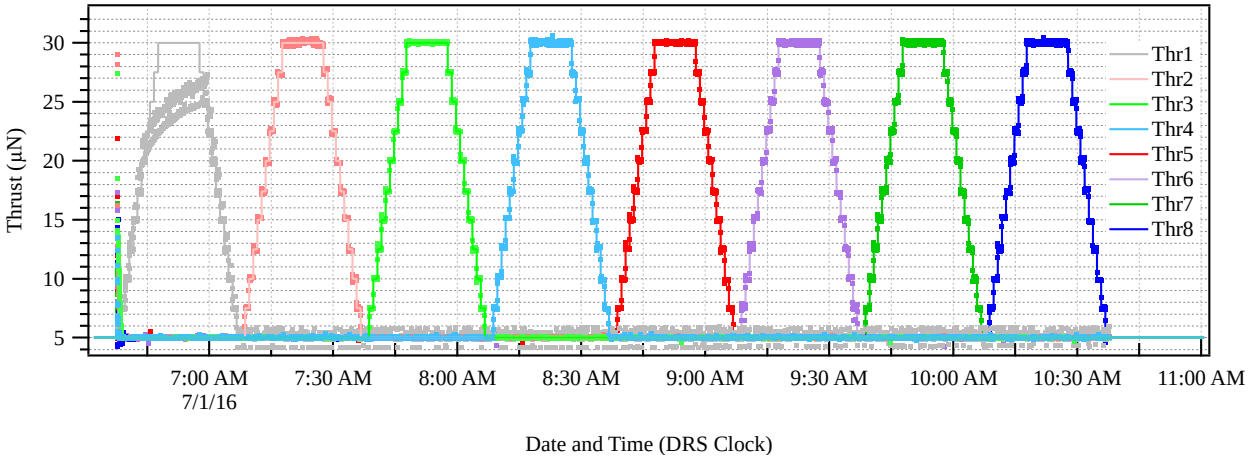

Figure 6. Commanded (solid lines) and delivered (dots) thrust for each of the 8 thrusters during a functional test to demonstrate 30 µN thrust range capability on one thruster at a time.

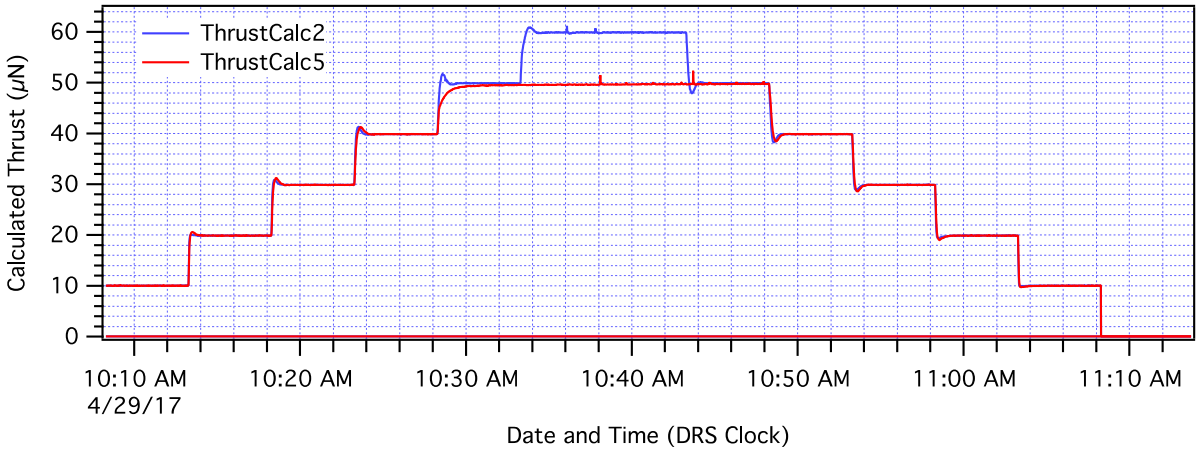

Figure 7. Higher thrust range demonstrated for thrusters 2 and 5 up to 50 and 60 µN.

D. Thrust Precision

The thrust precision met the 1σ requirement of 0.1 µN. Data in Figure 8 show the thrust precision control of thrusters 3 and 4. This precision was limited by the 12-bit A-D converter. The thrust precision could have been improved with a 16-bit converter.

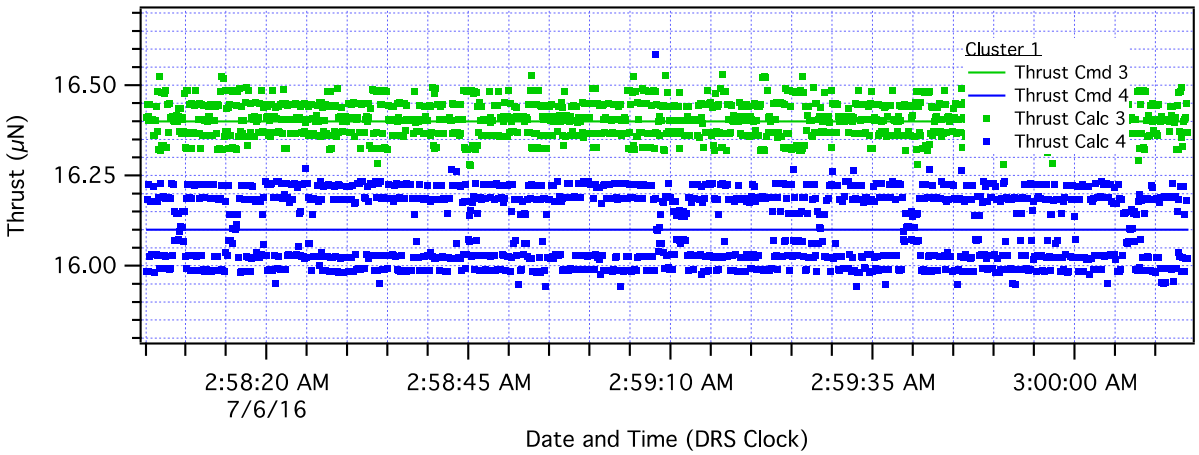

Figure 8. Data verifying required 0.1 μN thrust precision in Zero-G mode on DoY 188, July 6, 2016.

E. Thrust Response Time

The thruster response time met the requirement in steping from 5 to 30 μN in ≤10 s, for all of the thrusters except for thruster 1. Thruster 1 did achieve the full thrust range in ≤147 s in multiple tests. Thruster response time data are presented in Figure 9 from the commissioning phase of the mission. Thruster 3 and 7 increased from 5 to 30 μN in 8 s. Thrusters 2, 4, 5, 6, 8 increased from 5 to 30 μN in 10 s. Response times could be significantly reduced by changing parameters in the thruster control algorithm.

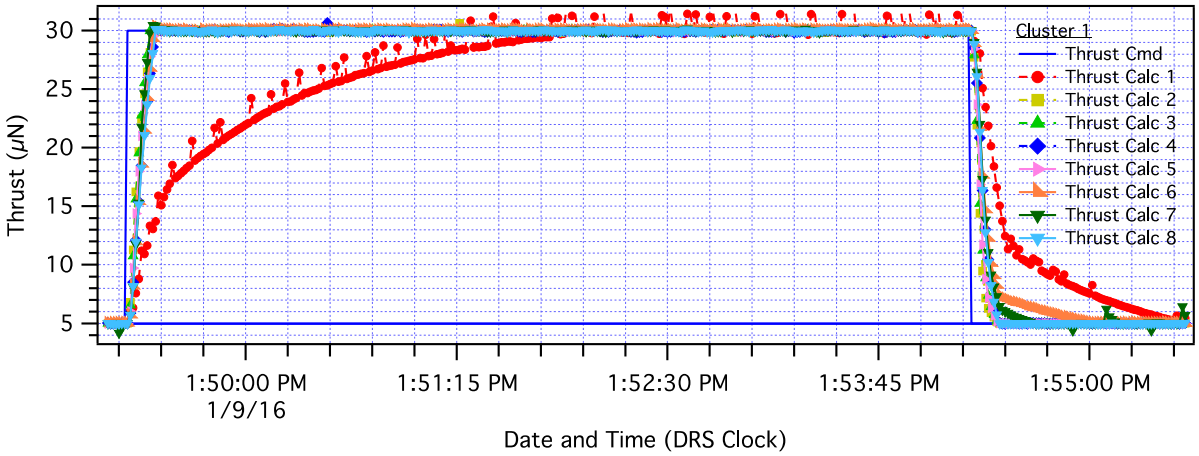

Figure 9. Data verifying thrust response time of ≤10 s for 5 to 30 μN, except for thruster 1 DoY 008 2016.

The DRS was required to control both the spacecraft attitude and position in several modes. The thrust commands and the thrust delivered, as calculated using the measured thruster voltages and currents and the thrust model, are in Figure 9 for each of the modes for 10 minutes on DoY 276 for thruster 3. The attitude error limit of 2° (35 mrad) was maintained in within the force and torque limits in all of the modes and transitions between them [2].

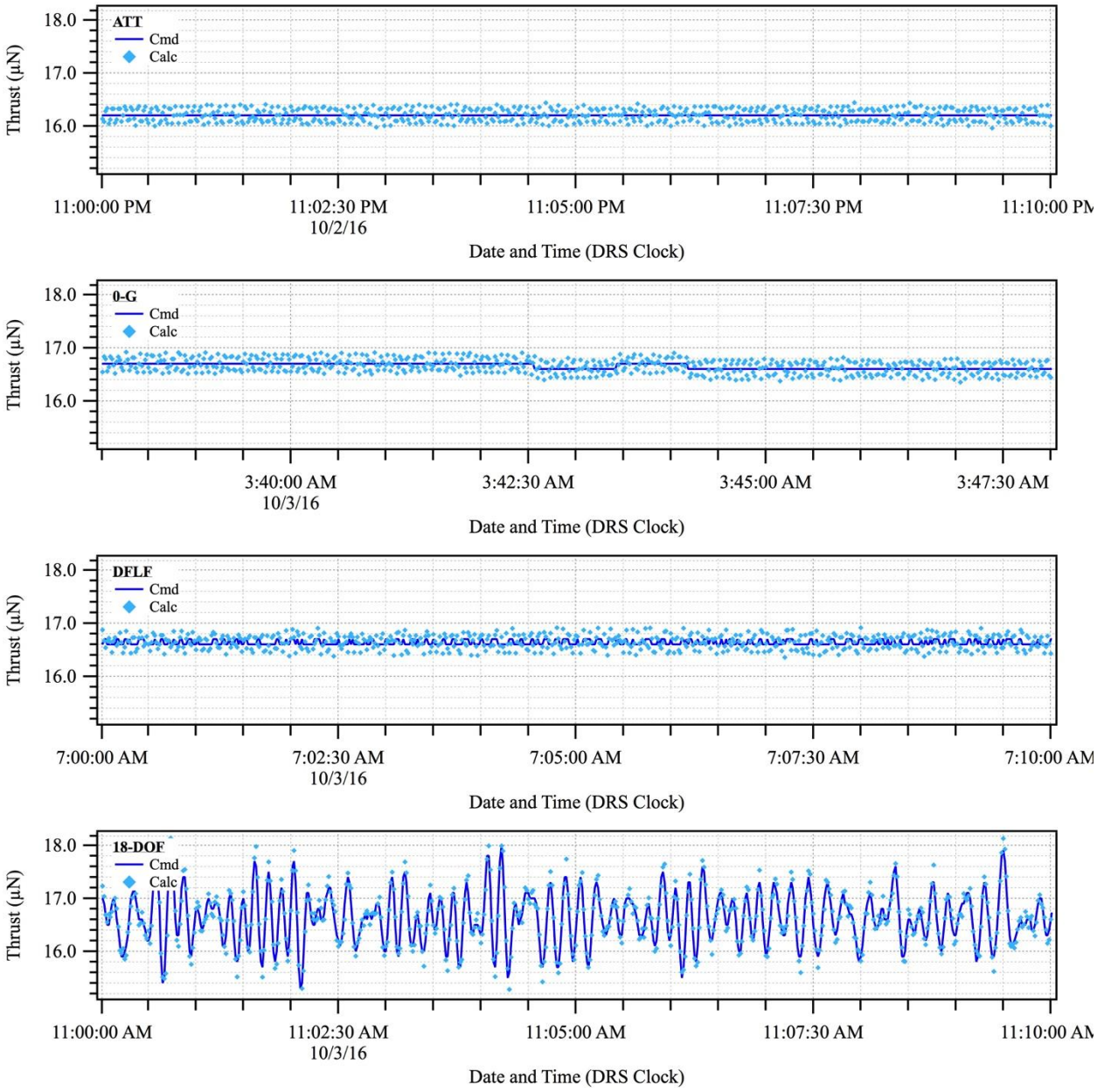

Figure 10. Commanded (solid dark blue line) vs calculated delivered thrust (lt. blue dots) in each mode (ATT, 0-G, DFLF, 18-DOF) for thruster 3 on DoY 277.

F. Thruster Noise

The requirement on thruster noise caps the average thruster disturbances within the DRS band. There are two top-level approaches to characterizing thruster noise on the spacecraft. The first is an open-loop characterization, which requires periods in which the thrusters are not used in the control of spacecraft, i.e., spacecraft is allowed to drift within the bounds of the Fault Management. The second approach involves characterization of thruster noise while the thrusters are used to provide actuation in the DCS controllers. This approach typically uses a pseudo-analytical model of thrust force to isolate thrust noise, and hence is model-dependent.

The open-loop characterization approach was chosen to verify the thruster noise requirement because it is direct and does not rely on a thrust model. Its use is further warranted since the thruster noise requirement applies to the Colloidal subsystem, and therefore, is an average, per thruster, specification. A thruster experiment (experiment T3) was conducted on DoY 245 (September 1, 2016), during which eight periods of free drifts were included. Prior to

each drift period, the thrust levels on the 8 thrusters were fixed at their last values in order to compensate for secular forces and torques, and hence maximize the allowed duration of the drift. In each drift period, a sinusoidal thruster injection (at 23mHz) is included for 1 of 8 thrusters to characterize other aspects of that thruster. This injection does not impact the noise characterization, as it is almost outside the band of interest, and it is narrow-banded. The T3 experiment was performed while the DRS was in the Zero-G mode, with the test masses serving as accelerometers.

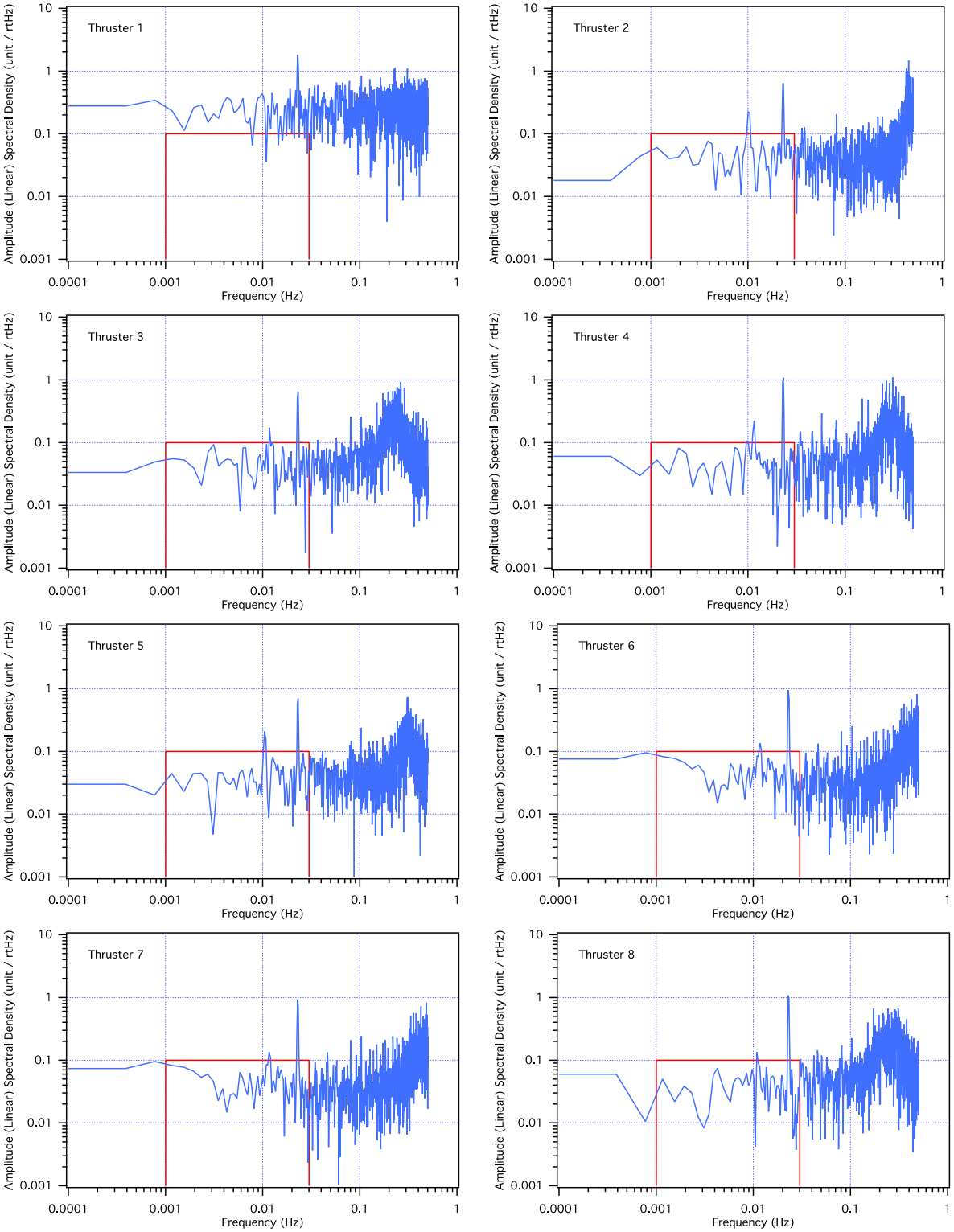

Figure 11. CMNT thrust noise in DFLF on DoY 245 over 2600 s with the requirement in the red box.

The thruster noise was characterized by calculating it for each thruster and then by measuring the collective thruster noise translated to the spacecraft. The individual thrust noise characterization is derived from the difference between the commanded thrust and the thrust calculated from the measured beam current and voltage using the thruster model. It is presented for the frequency range of interest for the LISA mission at 1 – 30 mHz for each of the thrusters in Figure 11. The requirement was ≤0.1 μN/√Hz at 1 -30 mHz, as indicated by the red box.

The spacecraft force noise was estimated by double differentiating the OMS data for each test mass along the sensitive axis (LPF data at 10Hz), subtracting the estimate of the applied ES force for each test mass, with appropriate scale factors (electrostatic force, ratio of S/C mass to mass of the test mass) and time delay, and finally averaging the force noise estimates from the two test masses. The amplitude spectral density of the spacecraft force noise, which is expected to be dominated by the colloidal thruster noise, averaged over the 8 thrusters, is shown and compared to the requirement in Figure 12. The average thrust noise meets the requirement with margin. The sharp peak at 23mHz is due to the thruster injection signal and should be ignored. The S/C force noise is cross checked by using the average estimates of the applied electrostatic force (adjusted for mass ratios and actuation scale factor) for the test masses. This cross check is limited to the effective bandwidth of the TM Accelerometer mode in Zero-G (~4 mHz). The results are presented in Figure 12, where a good match is observed.

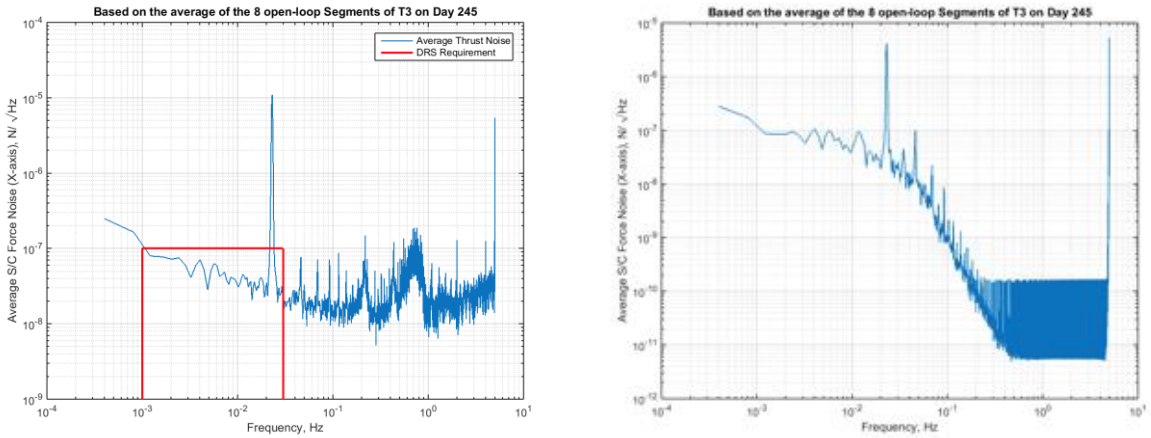

Figure 12. Amplitude spectral density of average thrust noise on the spacecraft. The red box shows DRS requirements, which are easily met. The graph on the right shows the amplitude of the average spacecraft force noise from electrostatic actuation commands only with the CNMTs off for comparison. [2]

G. Thruster Response to Disturbance Event

During the primary mission several disturbance events were observed that were suspected as having been micromteorite impacts. The impact of the disturbance on the test mass position and angle and the control system and thruster response to successfully recover the spacecraft attitude, position and angle errors are presented in Figure 13. The DRS was responsive enough to manage the disturbances and maintain the required spacecraft attitude error. Several of these events were observed during the mission at a frequency that was higher than expected.

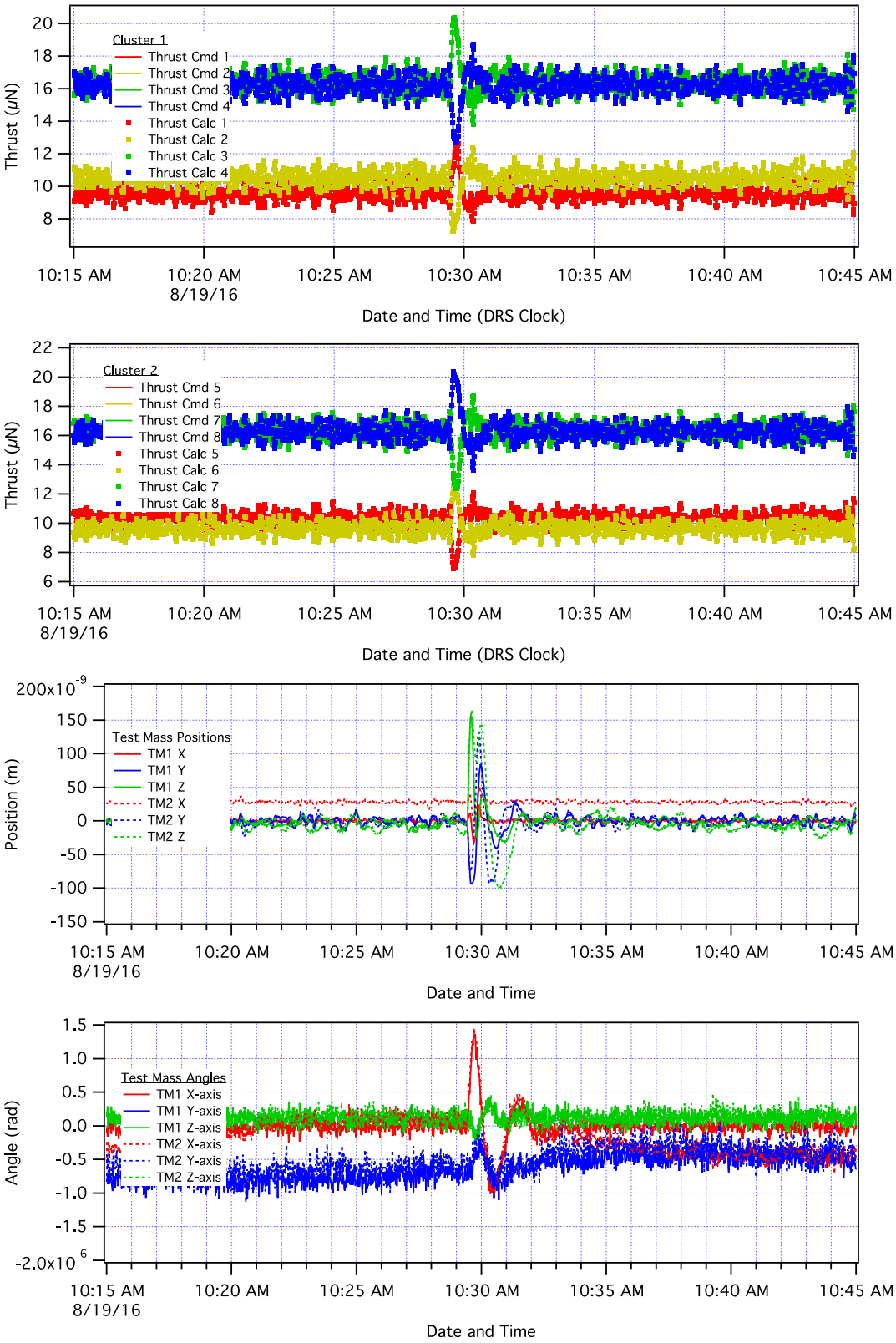

Figure 13. Response of all 8 thrusters and the test mass position and angle to an unknown disturbance event to stabilize the spacecraft attitude, position and angle on DoY 232, August 19, 2016.

IV. Carbon Nanotube Cathodes

The cathode on each thruster cluster was tested simultaneously in a thruster cluster current balancing mode. Each cluster with 4 thrusters has 1 carbon nanotube cathode that is capable of emitting electrons at a current level that is equivalent to the combined current level of all of the thrusters in that cluster. This test was conducted in diagnostic mode. Cathode data from the primary mission are in Figure14. The graph shows the voltage, beam current, and current to the cathode gate electrode. These data were sampled once per minute. The total thruster current for all thrusters in each cluster is also included in the graph. These data were sampled once minute. The peak total current from each cathode was ~14.8 µA. The gate current was ~4.9 µA. The current escaping from the cathode, beam current, was 9.9 µA. The beam current from each thruster was 2.5 µA and from each cluster was 10 µA at 12:07 pm. The cathode current balancing with the beam current was successful. Cathode 1 required 239 V. Cathode 2 required 473 V. This cathode test duration was about 16 minutes. The cathodes were tested again during the extended mission with 6 on-off cycles with independent control of cluster 1 and 2 cathodes. These data are in Figure 15. They show repeatable performance throughout the cycles. The cluster 1 cathode emitted 5.6 µA of beam current at 249 V and cluster 2 emitted 5.6 µA of beam current at 463 V. In TVAC tests, Cathode 1 required 243 V for 20 µA of total current with 12 µA of beam current escaping through the extractor. Cathode 2 required 372 V for 20 µA of total current and 12 µA of beam current in the TVAC tests.

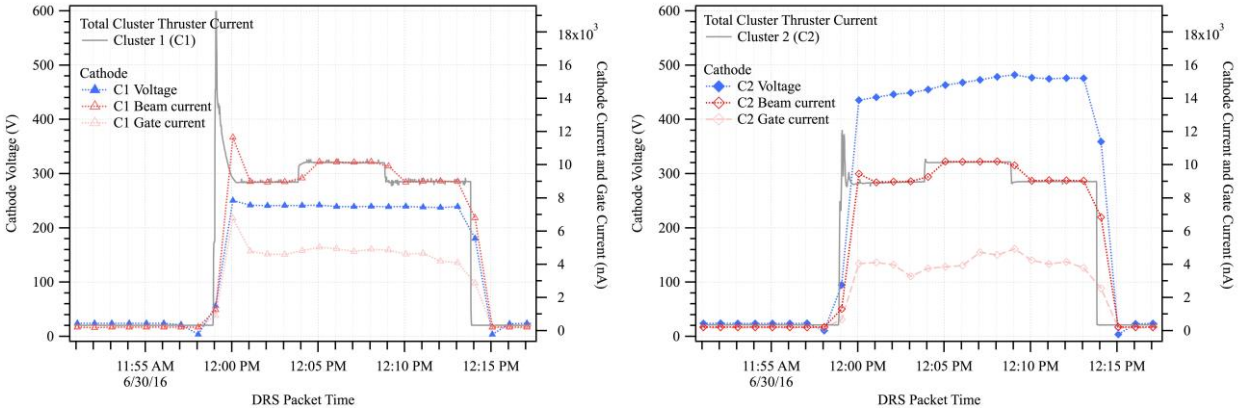

Figure 14. Cluster 1 (left) and Cluster 2 (right) cathode current and voltages while operating in a current balancing mode with the thruster clusters in the primary mission.

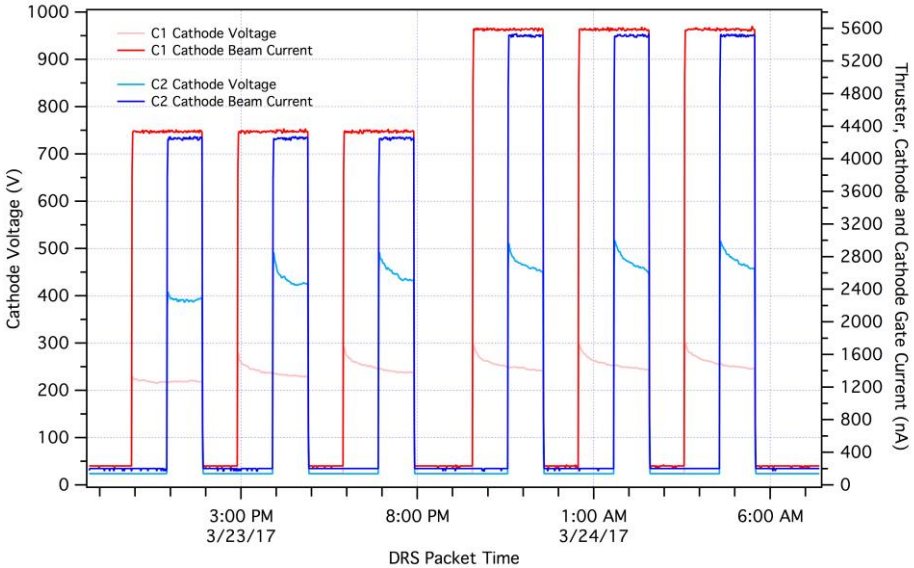

Figure 15. Cluster 1 (C1) and cluster 2 (C2) cathode beam current and voltages while operating in a current balancing mode with the thruster clusters in the extended mission for 6 cycles.

V. Anomolies

The DRS experienced 3 significant anomalies during the mission that affected operations; however, they did not prevent the mission from meeting the performance requirements. Thruster 1 demontstrated a delayed response time and a single flickering emitter throughout the primary and extended mission that was not observed during TVAC testing before delivery and launch. The DCIU EPROM suffered a partial failure in the location of the thruster control algorithm just after commissioning at the beginning of the primary mission. Thruster 4 experienced a short between the emitter and the extractor electrode near the end of the primary mission. The anomalies were addressed and solutions were developed to enable operations to continue through the extended mission.

A. Thruster 1

Thruster 1 performance in flight was not consistent with the TVAC tests on the ground before delivery and launch. In the TVAC tests, the response time was 9.8 s to increase from minimum to maximum thrust of 5 to 30 μN, as required. In flight, this thruster took longer than the other thrusters to turn on and initially had a response time of about 147 s. The requirement was 100 s. The response time increased during the mission, primarily for the first turn on after a prolonged period of being off. In flight, the beam current was also blipping up ~0.25 μA every few seconds, depending on the current level, throughout the entire mission. This behavior was not observed during TVAC testing. The delayed response time and blipping current indicated a change in hydraulic resistance of the thruster and performance of the valve. Experiments were conducted in the extended mission to try to improve the response time and characterize the current blipping to determine if there was a bubble in the thruster or particulate contamination and if the delayed response was attributable to a piezo valve element failure. The results suggest that the change in performance was not caused by a bubble. Particulate contamination in an emitter could have increased the hydraulic resistance to severely limit the flow rate and cause one of the emitters to blip on and off. A valve piezo element failure could have caused a reduced range of the valve and slow response. Both of these performance changes were observed at the same time, suggesting that they could be related. Because of the all of the other 7 valves performed the same in flight as on the ground, this anomaly may be a technology development yield issue that can be addressed by maturing the technology and/or flying redundant valves, as is common practice for science missions.

B. DCIU

The DCIU experienced an anomaly on July 8, 2017 that resulted in a processor reset and thruster cluster 2 being disabled when it received a thrust command. Testing revealed that while the Thrust Command Mode no longer functioned properly, the Diagnostic Mode did. The thruster control algorithm had to be executed in the FSW instead to prevent the reset because the DCIU processor had been damaged and could not be replaced or re-written. In this 'Diagnostic Mode' the FSW calculated the thruster current and voltages from the thrust commands using the thruster control algorithm, instead of the DCIU, and then passed them through the DCIU to the PPU. And old version of the thruster control algorithm that was in the FSW was modified as required, to enable this Diagnostic DCIU Pass-through Mode, and operations continued on August 8, 2016. The expected cause of this anomaly is a radiation event. A more robust and re-writable processor is recommended for future missions to prevent this type of anomaly. While this diagnostic mode approach created a timing delay in the control loop that resulted in noise on the beam voltage and increased thruster noise, the DRS met the noise requirements for the mission.

C. Thruster 4

Thruster 4 developed an electrical short between the emitter and extractor near the end of the primary mission that rendered it inoperable. The short was developed on Oct 27, 2016 after 1670 hours of operation. The resistance of the short was 200 MOhm. The location and configuration of the short cannot be determined without access to the thruster. It is suspected to be a propellant bridge between the emitter and extractor. This electrically conductive bridge could have formed when the extractor collected enough propellant to spray back to the emitter and become polymerized by the current and high energy charged particles. This anomaly may be partially attributable to an abbreviated thruster shutdown procedure that was adopted during SKM to shorten the procedure and preserve the spacecraft thermal environment at the request of ESA. The safe thruster shutdown procedure first includes closing the valve, which sucks back some of the residual propellant in the emitter capillary tubes from the emitter tips into a volume at the valve. Then the thrusters are heated up to 40°C for 1 hour to expand the propellant, and with electrode voltages applied, electrosprays to drain some of that residual propellant out of the emitters. In the abbreviated thruster shutdown procedure, they were not heated to 40°C to electrospray residual propellant out of the emitters and the electrode voltages remained applied for the SKM over a few days. Current flickering on and off at

0.05-0.25 µA level was observed, typically only from thruster 4, during these days as propellant was drawn out with voltage applied and electrosprayed. It seems likely that this flickering electrospray during the SKM contributed to the development of the propellant bridge, as this current could be sprayed between the emitter and extractor. This thruster also demonstrated more current flickering with the valve closed during TVAC testing before integration onto the spacecraft. It sprayed more charge in this flickering mode than any other of the thrusters. Determining how to prevent this current flickering when the valve is closed with more valve suckback and safe shutdown procedures will be critical to the further development of this thruster technology for future missions. Implementing redundant thruster heads will also be critical to future missions for the required lifetimes, as is common practice for science missions.

A hybrid (crutch) mode was developed to continue DRS operations with only 7 colloid thrusters and 4 of the LTP cold gas (CGAS) thrusters after the thruster 4 anomaly. The colloid thruster and cold gas thruster thrust bias levels and new handover procedures and sequences were developed also for this new operating mode. Both 4 and 2 CGAS thruster configuration were demonstrated on the test bed; however ,the 4 thruster configuration was preferred to reduce the required colloid thruster thrust bias levels. This hybrid mode was demonstrated just before the last week of the primary mission in all DCS modes and continued successfully through the extended mission, with higher force noise than the purely colloid thruster mode.

VI. Conclusion

The ST7-DRS payload on the LPF spacecraft successfully demonstrated two new technologies - Colloid Electrospray Thrusters (CMNT) and 18-degree-of-freedom drag free spacecraft control, while meeting mission performance requirements to enable future gravity wave observatories. It demonstrated the required performance in spacecraft attitude, position and drag-free control, validating the DCS and CMNT and performance models. It demonstrated the technologies that are also critical for separated element interferometers and telescopes and other applications needing extremely low position noise. Thrusters demonstrated the required performance in thrust range, precision, response time, noise and operating time. They operated in a thrust range of 5- 30 µN from 9 emitters with a response time <10 s and a precision better than 0.1 µN for over 2400 hours. Their performance in space was consistent with ground test results. Thrusters also demonstrated 50 and 60 µN thrust ranges. These colloid thrsuters could provide higher ranges of thrust by increasing the number of emitters in the head to accommodate various future mission applications and requirements, while maintaining the required thrust precision and noise. Significant thrust noise improvements, possibly by a factor of 10, are expected without the current blipping on thruster 1 and by improving the thrust resolution by replacing the 12 bit A-D converter with a 16 bit A-D converter. The thruster response time could be decreased by changing the control algorithm parameters. Minor technology improvements are expected to the propulsion system including sub-system redundancy and propellant tank volume to achieve multi-year lifetime requirements for missions like a gravity wave and exoplanet observatories. Carbon nanotube cathodes were also demonstrated during commissioning and then again during the extended mission in a thruster current balancing mode through several cycles with stable and repeatable performance. This mission validated this electrospray thruster technology for spaceraft attitude and drag-free control for exoplanet observatories.

Acknowledgments

The research described in this paper was carried out by the Jet Propulsion Laboratory, California Institute of Technology, Goddard Space Flight Center and Busek Co. under contract with the National Aeronautics and Space Administration and with extraordinary support from the LISA Pathfinder spacecraft and science teams, especially Jose Mendes and Ian Harrison at the European Space Agency.

References

1. M. Armano, et al. “Sub-Femto-g Free Fall for Space-Based Gravitational Wave Obervatories: LISA Pathfinder Results,” Physical Review Letters 116 231101 (2016).

2. P. G. Maghami, J.R. O'Donnell, O.H. Hsu, J.K. Ziemer, C.E.Dunn, "Drag-Free Performance of the ST7 Disturbance Reduction System Flight Experiment on the LISA Patfinder," GNC 2017: 10th International ESA Conference on Guidance, Navigation and Control Systems, 29 May-2 June 2017, Salzburg, Austria
3. Ziemer, J.K., Randolph, T.M., Franklin, G.W., Hruby, V., Spence, D., Demmons, N., Roy, T., Ehrbar, E., Zwalen, J., Martin, R., Connolly, W., "Delivery of Colloid Micro-Newton Theusters for the Space Technology 7 Mission," AIAA- 2008-4826, 44th AIAA/ASME/SAE/ASEE Joint Propulsion Conference & Exhibit, 21-23 July 2008, Hartford, CT.
4. Zwalen, V. Hruby, V, Campbell, C., Demmons, N., Ehrbar, E., Freeman, C., Martin, R., Roy, T., Spence, D., "Flow control Micro-valve for the ST7-DRS Colloid Thruster," AIAA-2008-4930, 44th AIAA Joint Propoulsion Conference, Hartford, CT, July 2008.
5. V. Hruby, et al, "Busek Colloid Thruster Development," *3rd Colloid Thruster Nano-Electrojet Workshop*, MIT, Boston, MA, April 14-15, 2005.
6. Ziemer, J.K., Randolph, T.M., Franklin, G.W., Hruby, V., Spence, D., Demmons, N., Roy, T., Ehrbar, E., Zwalen, J., Martin, R., Connolly, W., "Delivery of Colloid Micro-Newton Theusters for the Space Technology 7 Mission," AIAA- 2008-4826, 44th AIAA/ASME/SAE/ASEE Joint Propulsion Conference & Exhibit, 21-23 July 2008, Hartford, CT
7. J.K. Ziemer, T. M. Randolph, M. Gamero-Castano, V. Hruby, W. Connolly, N. Demmons, E. Ehrbar, R. Martin, T. Roy, " Flight Hardware Development of Colloid Microthruster Technology for the Space Technology 7 and LISA Mission," IEPC 2007-288, 30th International Electric Propulsion Conference, Florence, Italy, September 17-20, 2007.
8. N. Demmons, et. al., "ST7-DRS Mission Colloid Thruster Development," AIAA-2008-4823, 44th AIAA Joint Propulsion Conference, Hartford, CT, July 2008.
9. Hruby, et al, "Neutralizers for Electric Micro-propulsion Thrusters," 44th AIAA Joint Propoulsion Conference, Hartford, CT, July 2008.
10. E. Ehrbar, et al, "Power Processor for the Colloid Micro-Newton Thruster," 44th AIAA Joint Propulsion Conference, Hartford, CT, July 2008.